Altering the Superconductor Transition Temperature by Domain-Wall Arrangements in Hybrid Ferromagnet-Superconductor Structures

L. Y. Zhu, T. Y. Chen, and C. L. Chien*

Department of Physics and Astronomy, Johns Hopkins University, Baltimore, Maryland 21218, USA

(Received 22 December 2007; published 3 July 2008)

The $[Co/Pt]_n/Nb/[Co/Pt]_n$ hybrids with perpendicular magnetic anisotropy reveal enhanced superconductivity with the presence, and the arrangements, of domain walls, where superconductivity persists. An in-plane field can manipulate the domain walls from labyrinth to stripe patterns and drive the hybrids from normal to superconducting. We observe anisotropic superconductivity in hybrids with stripe domains, along which enhanced superconductivity is realized.

DOI: 10.1103/PhysRevLett.101.017004 PACS numbers: 74.78.Fk, 74.62.−c, 75.60.Ch

Ferromagnet-superconductor (F-S) hybrid structures have attracted extensive theoretical and experimental attention due to the coexistence of two antagonistic phenomena: spin alignment in ferromagnets and Cooper pairs of opposite spins in superconductors. A variety of novel phenomena have been reported in F-S hybrids [1–17], such as the spin switch effect [3–10] and the domain-wall superconductivity [1,2,8,12–16]. In the latter, in both bilayers and trilayers, the transition temperature T_c of the S layer depends on the appearance of domain walls in the F layer during magnetization reversal, an effect attributed to the lowered average exchange field sensed by the Cooper pairs in the domain-wall region. Thus far, most such studies have utilized ferromagnets with in-plane magnetic anisotropy, such as Ni and Py with large domain sizes and not well-defined domain patterns. In contrast, ferromagnets with perpendicular magnetic anisotropy (PMA), such as Co/Pt multilayers, not only acquire magnetization perpendicular to the F-S interfaces but also display much smaller domain sizes, allowing pronounced effects for the domain-wall superconductivity. Equally important, the domain patterns in ferromagnets with PMA can be controlled by an in-plane magnetic field [18].

We show in this work using F-S and F-S-F hybrids with PMA that, while the appearance of domain walls enhances superconductivity, the *arrangement* of domain walls shows even greater influence. By manipulating the domain patterns in the F layer between parallel stripes and random labyrinth, the S layer can be driven between the superconducting state and the normal state at the same temperature and magnetic field. The hybrids are even more superconducting in a magnetic field with the presence of parallel stripe domains than that without the field. These results show that the superconductivity of F-S hybrids occurs in the domain-wall region, which provides the superconducting pathways.

We first describe the results of $[Co6/Pt15]_4/Nb380/[Co4/Pt11]_4$, an F-S-F trilayer consisting of a superconducting Nb sandwiched between two Co/Pt multilayers with PMA with thickness denoted in angstroms. At 10 K, which is above the T_c of 4.835 K, the hysteresis loop of the sample [Fig. 1(a)] in an out-of-plane magnetic field $H_\perp$ shows that the top $[Co4/Pt11]_4$ and bottom $[Co6/Pt15]_4$ stacks have different switching fields of $H_c^t = 400$ Oe and $H_c^b = 580$ Oe, respectively, which can be identified by the magnetization reversal. As shown in Fig. 1(b), the resistance (R) of the sample at 4.830 K increases with $|H_\perp|$ and becomes normal at $|H_\perp| > 1$ kOe. However, there are two sharp resistance dips when sweeping $H_\perp$ in either direction at ± 410 and ± 590 Oe, which are close to the switching fields of $\pm H_c^t$ and $\pm H_c^b$, respectively. The dips in R occur at *both* H_c^t and H_c^b, when the top and the bottom Co/Pt multilayers switch separately. Indeed, only one set of dips has been observed in our $[Co/Pt]_n/Nb$ bilayer hybrids (not shown). In a sample of $[Co/Pt]_n/Si/Nb$ with an 89 Å insulating Si layer between the Nb and the Co/Pt multilayers, no resistance dips were found during magnetization reversal. These results clearly show that a stray field cannot be a viable cause. Instead, they show that the enhanced superconductivity manifested by the sharp dips in R is due to the presence of domain walls during magnetization switching, in which the Cooper pairs experience weaker proximity exchange field and hence weaker pair-breaking effects.

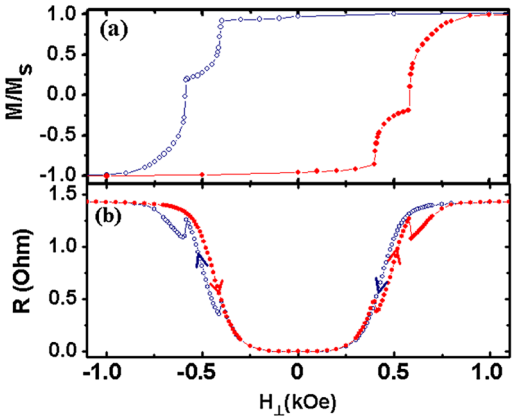

FIG. 1 (color online). (a) Normalized magnetization M/M_s at 10 K and (b) resistance R at 4.830 K versus out-of-plane magnetic field $H_\perp$ for $[Co6/Pt15]_4/Nb380/[Co4/Pt11]_4$ with thickness in angstroms, where the top $[Co4/Pt11]_4$ and the bottom $[Co6/Pt15]_4$ switch at ± 400 and ± 580 Oe, respectively.

However, a completely different behavior is observed when the $[Co6/Pt15]_4/Nb380/[Co4/Pt11]_4$ was measured with an in-plane field $H_{\|}$ as shown in Fig. 2(a) at 4.785 K. Following the decreasing $H_{\|}$ branch (blue squares) from +5 kOe, R initially decreases, reaches a minimum at 0.6 kOe and then increases, with a corresponding behavior on the increasing $H_{\|}$ branch (red circles). However, comparing the results between Fig. 2(a) with $H_{\|}$ and Fig. 1(b) with $H_{\perp}$, one immediately notes that in the positive field range with $H_{\|}$ [Fig. 2(a)] the resistance R in the field-increasing branch is higher than that in the field-decreasing branch. Exactly the opposite has been observed for $H_{\perp}$ [Fig. 1(b)], suggesting the connection with the actual domain patterns.

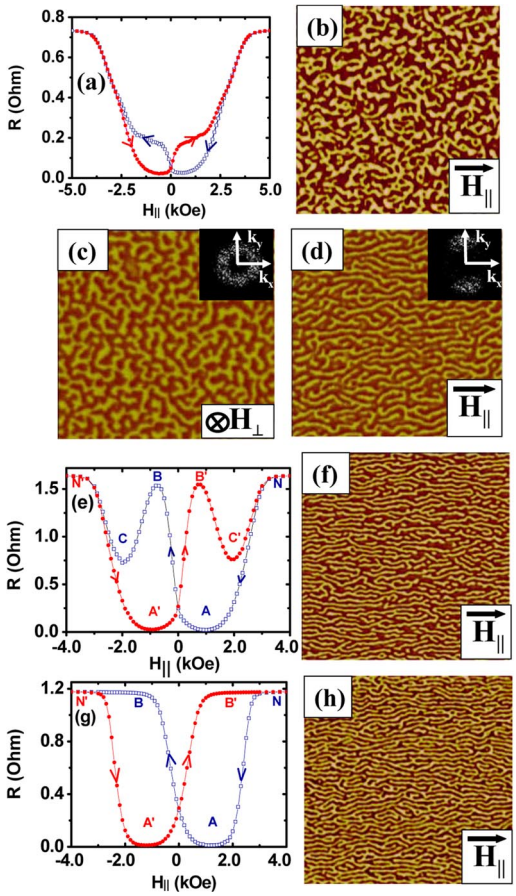

FIG. 2 (color online). (a) Resistance R versus in-plane field $H_{\|}$ at 4.785 K and (b) MFM image after in-plane demagnetization of the sample shown in Fig. 1 with slightly different dimensions. MFM image of the *in situ* field-deposited $[Co6/Pt15]_4/Nb380/[Co4/Pt11]_4$ sample with (c) a labyrinth domain after out-of-plane demagnetization and (d) stripe domains after in-plane demagnetization. The upper right insets are 2D FFT spectrums of MFM images. Resistance R versus $H_{\|}$ for *in situ* field-deposited $[Co6/Pt15]_n/Nb560/[Co6/Pt15]_n$ sample, with (e) $n = 8$ measured at 6.970 K and (g) $n = 25$ measured at 6.340 K, and their MFM images (f) and (h), respectively, after in-plane demagnetization. All MFM images are 10 μm × 10 μm taken at room temperature.

To clearly establish the connection between the superconducting behavior of the F-S-F trilayers with the domain structures, we fabricated the F-S-F trilayers of the same structure in an *in situ* magnetic field of about 120 Oe applied in the sample plane during deposition in order to induce a weak in-plane uniaxial anisotropy. The effect of the small deposition field in the field-deposited (FD) samples does not alter the overall PMA but drastically alters the domain patterns as revealed by magnetic force microscopy (MFM) at room temperature shown in Fig. 2. After demagnetizing with an out-of-plane ac magnetic field $H_{\perp}$, the FD sample shows a labyrinth domain pattern with an average domain width of about 230 nm [Fig. 2(c)]. In contrast, after the in-plane $H_{\|}$ demagnetization along the deposition field direction, the same FD sample exhibits largely parallel stripe domains along $H_{\|}$ with an average domain width of about 140 nm [Fig. 2(d)], instead of the nearly random maze pattern in the same multilayer structure but deposited without the *in situ* field [Fig. 2(b)].

The hysteresis loop of the FD sample at 10 K and the magnetoresistance (MR) at 5.350 K in an in-plane field $H_{\|}$ along the deposition field direction are shown in Figs. 3(a) and 3(b), respectively. The magnetization (M) increases monotonically with $H_{\|}$ and acquires in-plane magnetization at 4 kOe, whereas the MR shows unusual nonmonotonic field dependence. Starting from +4 kOe (point N) with decreasing $H_{\|}$, R decreases to a minimum at 0.8 kOe (point A), a local maximum at −0.4 kOe (point B), and another minimum at −1.4 kOe (point C) before it saturates at −4 kOe (point N'). The same behavior is also observed for the increasing field branch, from N' to A', B', C', and N. There is a large difference in resistance between the increasing and the decreasing $H_{\|}$ branches. This aspect can be illustrated in the temperature scan at a constant magnetic field as shown in Fig. 3(c) at $H_{\|} = 4$ (the saturation state), 0 (the remnant state), 0.5 (increased from −10 kOe), and 0.5 kOe (decreased from +10 kOe). The value of T_c at $H_{\|} = 0$ is higher than that at $H_{\|} = 4$ kOe as expected. However, the two scans at $H_{\|} = 0.5$ kOe are very different; the sample exhibits the highest T_c at 0.5 kOe (decreased from +10 kOe), higher even than that at $H = 0$. As described below, these results cannot be solely explained by the appearance of domain walls in the F layer.

It is known [1,2] that the appearance of domain walls can induce superconductivity such as that shown in Fig. 1 with $H_{\perp}$ field. However, the results with $H_{\|}$ show that the *appearance* of the domain walls is not as essential as the *arrangement* of the domain walls. In materials with PMA, the number of domain walls increases during reversal and reaches the maximum at $M = 0$. As shown in Fig. 3(a), at the field of 0.4 kOe, the state point B'' has higher magnetization and fewer domain walls and hence is expected to be less superconducting than that at B', exactly opposite to that observed in Fig. 3(b). These results demonstrate clearly the more crucial role of domain pattern in the superconductivity of the F-S hybrids.

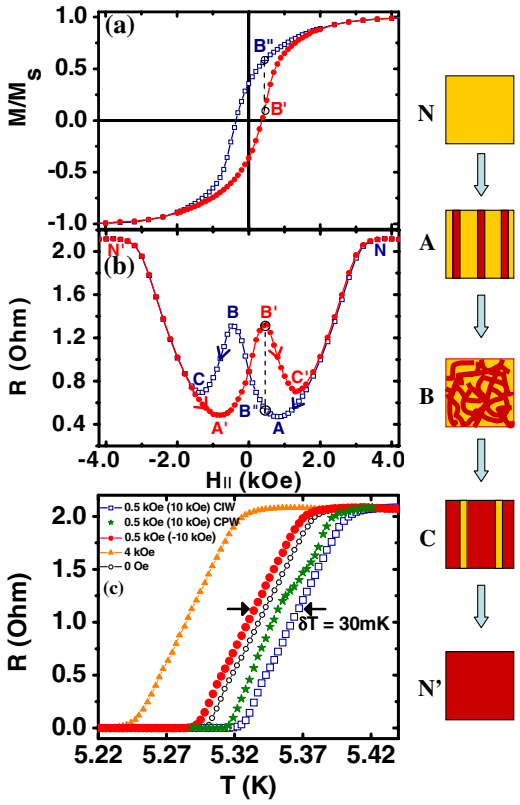

FIG. 3 (color online). (a) Normalized magnetization M/M_s at 10 K and (b) resistance R at 5. 350 K versus in-plane magnetic field $H_{\|}$ for the *in situ* field-deposited $[Co6/Pt15]_4/Nb380/[Co4/Pt11]_4$ sample. Points B' and B'' are at the same magnetic field illustrated by vertical dashed lines. (c) Resistance R versus temperature T of the same sample at 4 (in-plane saturation field, solid triangles), 0 (remnant state, open circles), 0.5 with measuring current parallel (CIW, open squares) and perpendicular (CPW, solid stars) to stripe domains (both reduced from +10 kOe), and 0.5 kOe (increased from −10 kOe, solid circles). The domain structure evolution is schematically shown on the right.

Because the domain-wall regions are more superconducting (and hence less resistive) than the domain regions, the total resistance depends on the manner with which these two components are interconnected as defined by the domain pattern. For the stripe domain arrangement, since the measuring current is along the stripe direction, the resistances due to the domain walls and the domains are connected *in parallel*. As such, the smaller resistance of the domain walls dominates the total resistance. In contrast, for the labyrinth domains, the 2D fast Fourier transform (FFT) spectrum in the inset in Fig. 2(c) shows a ring pattern indicating an isotropic domain-wall arrangement. The domain wall and the domain regions are randomly mixed, resulting in a higher total resistance. The complex MR behavior shown in Fig. 3(b) is due to the evolution of the domain pattern as a result of $H_{\|}$ as schematically shown on the right of Fig. 3. Following the decreasing field branch from point N at $H_{\|} = 4$ kOe with an in-plane single domain, with decreasing $H_{\|}$, the reversed domains gradually appear along $H_{\|}$, and R decreases and reaches the lowest resistance at point A when the most ordered parallel stripe domains appear. Upon further decreasing $H_{\|}$, the out-of-plane component of magnetization increases, and the stripe domains give way to the random labyrinth domains at point B. Beyond that, $H_{\|}$ begins to realign the stripe domains with the opposite polarity, resulting in decreasing R with a minimum at point C. After that, the increasing field eventually removes all stripe domains. One notes that different superconducting properties along or perpendicular to the stripes are expected in the stripe domain. This anisotropic superconductivity can be explored by measuring T_C along and perpendicular to the stripes. Indeed, the T_C measured perpendicular to the stripes is lower than that measured along the stripes, as shown by the solid stars in Fig. 3(c). We emphasize that the anisotropic superconductivity, due to the unique stripe domain structure acquired in the F-S hybrids with PMA, is not detectable in hybrids with in-plane anisotropy [19]. Theoretical calculations have shown that a stripe domain wall in F-S hybrids can guide the movement of vortices, thus resulting in anisotropic superconducting transport [20,21]. This is a likely underlying mechanism in our F-S hybrids.

The stripe domains of the FD samples in $[Co/Pt]_n$ stacks with a higher n become even better defined with a concomitant effect on superconductivity as illustrated in $[Co6/Pt15]_n/Nb560/[Co6/Pt15]_n$, with $n = 8$ and 25. After $H_{\|}$ demagnetization, the MFM image in Figs. 2(f) and 2(h) shows better aligned parallel stripes along the external demagnetization field than that of $n = 4$ [Fig. 2(d)] as well as larger resistance differences between the more superconducting parallel stripe domain state (points A and A') and the less superconducting random labyrinth domain state (points B and B') by comparing Figs. 2(e), 2(g), and 3(b). In fact, as shown in Fig. 2(e), the sample can be switched between completely superconducting (point A) and normal (point B') at the *same* temperature and magnetic field, demonstrating the relationship between the arrangement of domain walls and superconductivity. The dip at point C or C' in Figs. 2(e) and 3(b) disappears in Fig. 2(g), because the weakening PMA of $[Co/Pt]_n$ with increasing n cannot form stripe patterns from B to C as shown on the right of Fig. 3.

Results in Fig. 1 show that superconductivity is enhanced by the appearance of the domain walls in the F-S hybrid with PMA under $H_{\perp}$. However, the domain-wall arrangements controlled by $H_{\|}$ display a much stronger effect on superconductivity. As shown in Fig. 3(c), T_c enhancement of 30 mK, much larger than the 10 mK previously observed [1], has been realized by controlling just the domain-wall arrangements. The two competing effects of appearance and arrangement of domain walls can be better revealed by the angular MR measurements at $T = 5.800$ K from in-plane and along the FD direction ($\theta = 0°$) to out of the plane ($\theta = 90°$). As shown in Figs. 4(a)–4(e), the shape of the MR curve, particularly

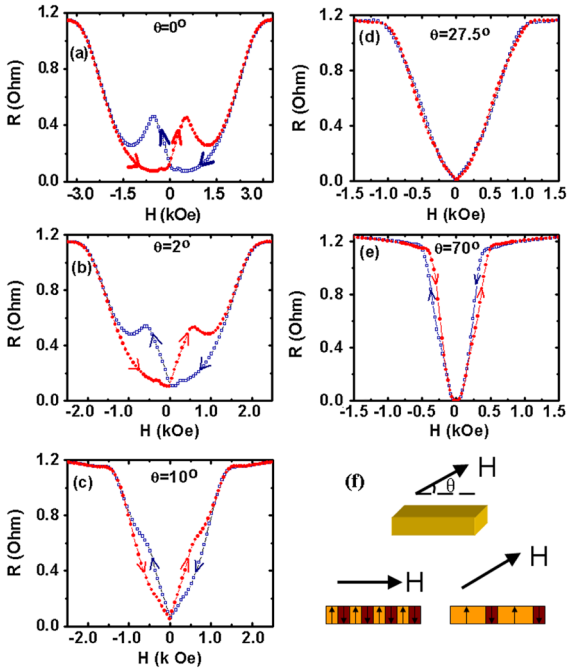

FIG. 4 (color online). Resistance versus field H with different field angle θ: (a) 0°, (b) 2°, (c) 10°, (d) 27.5°, and (e) 70° at 5.800 K for the *in situ* field-deposited $[Co6/Pt15]_4/Nb380/[Co4/Pt11]_4$ sample. (f) Schematic magnetic configurations for different field angles.

the peak at point B and dip at point C, depends sensitively on θ. These results indicate that the in-plane field is crucial in forming the stripe domain patterns. The effects of H on the magnetic domains are schematically shown in Fig. 4(f). At $\theta = 0°$ with only an in-plane field, a maximum number of domain walls are formed while H decreasing. With H at an angle θ, there are preferentially larger up domains and fewer domain walls than before. It is increasingly more difficult to alter the domain pattern between the more superconducting state with stripe domains and the less superconducting state with maze domains. This accounts for the gradual disappearance of the resistance peak at point B and the dip at point C. One also notes that for $\theta < 27.5°$ the decreasing H branch lies below the increasing H branch in positive H [Figs. 4(a)–4(c)] due to the formation of the stripe domain patterns. At larger angles $\theta > 27.5°$, e.g., $\theta = 70°$, the effect of the domain walls surpasses that of the domain patterns; thus, the two branches reverse their roles [Fig. 4(e)]. At $\theta \approx 27.5°$ [Fig. 4(d)], the two branches nearly coincide, and the nonhysteretic R-H behavior is similar to that of a single Nb thin film.

The observed superconducting behaviors in the F-S-F hybrids with PMA are intimately connected with the specific domain patterns. These are not trilayer effects but single F-S interface effects. Indeed, we have observed qualitatively similar effect in F-S bilayers with PMA, albeit the effects are significantly weaker than those in the F-S-F trilayers with two F-S interfaces [22].

In conclusion, we show that the superconductivity in F-S hybrids with perpendicular magnetic anisotropy persists at the domain-wall region. As such, the manipulation of the domain walls can greatly affect the superconducting properties of the hybrids, causing the hybrids to be superconducting or normal at the same temperature and external field. Anisotropic superconducting properties are realized in the F-S hybrids by the formation of stripe domains with an in-plane field.

This work has been supported by NSF Grants No. DMR05-20491 and No. DMR04-03849.

*Corresponding author.

[1] A. Yu. Rusanov, M. Hesselberth, J. Aarts, and A. I. Buzdin, Phys. Rev. Lett. **93**, 057002 (2004).
[2] M. Houzet and A. I. Buzdin, Phys. Rev. B **74**, 214507 (2006).
[3] L. R. Tagirov, Phys. Rev. Lett. **83**, 2058 (1999).
[4] J. Y. Gu, C. Y. You, J. S. Jiang, J. Pearson, Ya. B. Bazaliy, and S. D. Bader, Phys. Rev. Lett. **89**, 267001 (2002).
[5] I. C. Moraru, W. P. Pratt, Jr., and N. O. Birge, Phys. Rev. Lett. **96**, 037004 (2006).
[6] I. C. Moraru, W. P. Pratt, Jr., and N. O. Birge, Phys. Rev. B **74**, 220507(R) (2006).
[7] A. Potenza and C. H. Marrows, Phys. Rev. B **71**, 180503(R) (2005).
[8] A. Y. Rusanov, S. Habraken, and J. Aarts, Phys. Rev. B **73**, 060505(R) (2006).
[9] A. Singh, C. Sürgers, and H. v. Löhneysen, Phys. Rev. B **75**, 024513 (2007).
[10] R. Steiner and P. Ziemann, Phys. Rev. B **74**, 094504 (2006).
[11] J. Fritzsche, V. V. Moshchalkov, H. Eitel, D. Koelle, R. Kleiner, and R. Szymczak, Phys. Rev. Lett. **96**, 247003 (2006).
[12] W. Gillijns, A. Yu. Aladyshkin, M. Lange, M. J. Van Bael, and V. V. Moshchalkov, Phys. Rev. Lett. **95**, 227003 (2005).
[13] Z. Yang, M. Lange, A. Volodin, R. Szymczak, and V. V. Moshchalkov, Nat. Mater. **3**, 793 (2004).
[14] D. Stamopoulos and M. Pissas, Phys. Rev. B **73**, 132502 (2006).
[15] A. I. Buzdin and A. S. Mel'nikov, Phys. Rev. B **67**, 020503(R) (2003).
[16] T. Champel and M. Eschrig, Phys. Rev. B **71**, 220506(R) (2005).
[17] V. Pena, Z. Sefrioui, D. Arias, C. Leon, J. Santamaria, J. L. Martinez, S. G. E. te Velthuis, and A. Hoffmann, Phys. Rev. Lett. **94**, 057002 (2005).
[18] O. Hellwig, G. P. Denbeaux, J. B. Kortright, and Eric E. Fullerton, Physica (Amsterdam) **336B**, 136 (2003).
[19] C. Visani, V. Pena, J. Garcia-Barriocanal, D. Arias, Z. Sefrioui, C. Leon, J. Santamaria, N. M. Nemes, M. Garcia-Hernandez, J. L. Martinez, S. G. E. te Velthuis, and A. Hoffmann, Phys. Rev. B **75**, 054501 (2007).
[20] M. Amin Kayali and Valery L. Pokrovsky, Phys. Rev. B **69**, 132501 (2004).
[21] Serkan Erdin, Igor F. Lyuksyutov, Valery L. Pokrovsky, and Valeri M. Vinokur, Phys. Rev. Lett. **88**, 017001 (2001).
[22] L. Y. Zhu, T. Y. Chen, and C. L. Chien (unpublished).